

# UCLA

## UCLA Previously Published Works

### Title

Mechanism and Enantioselectivity in Palladium-Catalyzed Conjugate Addition of Arylboronic Acids to  $\beta$ -Substituted Cyclic Enones: Insights from Computation and Experiment

### Permalink

<https://escholarship.org/uc/item/36t4b8h9>

### Journal

Journal of the American Chemical Society, 135(40)

### ISSN

0002-7863

### Authors

Holder, Jeffrey C  
Zou, Lufeng  
Marziale, Alexander N  
[et al.](#)

### Publication Date

2013-10-09

### DOI

10.1021/ja401713g

Peer reviewed

Published in final edited form as:

*J Am Chem Soc.* 2013 October 9; 135(40): . doi:10.1021/ja401713g.

## Mechanism and Enantioselectivity in Palladium-Catalyzed Conjugate Addition of Arylboronic Acids to $\beta$ -Substituted Cyclic Enones: Insights from Computation and Experiment

 Jeffrey C. Holder<sup>†</sup>, Lufeng Zou<sup>‡</sup>, Alexander N. Marziale<sup>†</sup>, Peng Liu<sup>‡</sup>, Yu Lan<sup>‡</sup>, Michele Gatti<sup>†</sup>, Kotaro Kikushima<sup>†</sup>, K. N. Houk<sup>‡,\*</sup>, and Brian M. Stoltz<sup>†,\*</sup>
<sup>†</sup>The Warren and Katharine Schlinger Laboratory for Chemistry and Chemical Engineering, Division of Chemistry and Chemical Engineering, California Institute of Technology, Pasadena, California 91125, United States

<sup>‡</sup>Department of Chemistry and Biochemistry, University of California, Los Angeles, California 90095, United States

### Abstract

Enantioselective conjugate additions of arylboronic acids to  $\beta$ -substituted cyclic enones have been reported previously from our laboratories. Air and moisture tolerant conditions were achieved with a catalyst derived *in situ* from palladium(II) trifluoroacetate and the chiral ligand (*S*)-*t*-BuPyOx. We now report a combined experimental and computational investigation on the mechanism, the nature of the active catalyst, the origins of the enantioselectivity, and the stereoelectronic effects of the ligand and the substrates of this transformation. Enantioselectivity is controlled primarily by steric repulsions between the *t*-Bu group of the chiral ligand and the  $\alpha$ -methylene hydrogens of the enone substrate in the enantiodetermining carbopalladation step. Computations indicate that the reaction occurs via formation of a cationic arylpalladium(II) species, and subsequent carbopalladation of the enone olefin forms the key carbon-carbon bond. Studies of non-linear effects and stoichiometric and catalytic reactions of isolated (PyOx)Pd(Ph)I complexes show that a monomeric arylpalladium-ligand complex is the active species in the selectivity-determining step. The addition of water and ammonium hexafluorophosphate synergistically increases the rate of the reaction, corroborating the hypothesis that a cationic palladium species is involved in the reaction pathway. These additives also allow the reaction to be performed at 40 °C and facilitate an expanded substrate scope.

### Introduction

Asymmetric conjugate addition has become a familiar reaction manifold in the synthetic chemists' repertoire.<sup>1</sup> Though seminal reports involved highly reactive organometallic nucleophiles,<sup>2</sup> systems were rapidly developed that involved functional-group-tolerant organoboron nucleophiles. Namely, Hayashi pioneered the use of rhodium/BINAP catalysts for the asymmetric conjugate addition of a number of boron-derived nucleophiles.<sup>3</sup> As an economical alternative to the rhodium systems, Miyaura pioneered the use of chiral palladium-phosphine catalysts to address similar transformations<sup>4</sup> and Minnaard reported a palladium-catalyzed asymmetric conjugate addition using a catalyst formed *in situ* from palladium trifluoroacetate and commercially available (*S,S*)-MeDuPhos.<sup>5</sup>

\*Corresponding Author: stoltz@caltech.edu; houk@chem.ucla.edu.

Supporting Information. Experimental details, optimized Cartesian coordinates and energies, and complete reference of Gaussian 03. This material is available free of charge via the Internet at <http://pubs.acs.org>.

More recently, asymmetric conjugate addition has become a useful strategy for the challenge of constructing asymmetric quaternary stereocenters.<sup>6</sup> Again, many earlier developed methods involved highly reactive diorganozinc,<sup>7</sup> triorganoaluminum,<sup>8</sup> and organomagnesium<sup>9</sup> nucleophiles, however, more recently chiral rhodium/diene systems have been shown to construct asymmetric quaternary stereocenters with functional group-tolerant organoboron nucleophiles.<sup>10</sup> While rhodium systems are highly developed and exhibit a wide substrate scope, the high cost of the catalyst precursors and oxygen sensitivity of the reactions are undesirable. Despite progress in palladium-catalyzed conjugate additions for the formation of tertiary stereocenters,<sup>11</sup> no conditions were amenable to the synthesis of even *racemic* quaternary centers until Lu and coworkers disclosed a dicationic, dimeric palladium/bipyridine catalyst in 2010.<sup>12</sup> However, it was not until our recent report that a palladium-derived catalyst was employed to generate an asymmetric quaternary stereocenter *via* conjugate addition chemistry.<sup>13</sup>

We employed a catalyst derived *in situ* from Pd(OCOCF<sub>3</sub>)<sub>2</sub> and a chiral pyridinooxazoline (PyOx) ligand,<sup>14</sup> (*S*)-*t*-BuPyOx (ligand **1**, Scheme 1). This catalyst facilitates the asymmetric conjugate addition of arylboronic acids to β-substituted enones in high yield and good enantioselectivity. Importantly, this reaction is highly tolerant of air and moisture, and the chiral ligand, while not yet commercially available, is easily prepared.<sup>15</sup> Initial results with the Pd/PyOx system were reported rapidly due to concerns over competition in the field. Indeed, recent publications prove palladium-catalyzed conjugate addition to be a burgeoning field of research.<sup>16</sup> After the initial disclosure, we observed that in addition to catalyzing conjugate additions to 5-, 6-, and 7-membered enones, the Pd/PyOx catalyst successfully reacted with chromones and 4-quinolones.<sup>17</sup> Intrigued by the broad substrate scope and operational simplicity of this highly asymmetric process, we conducted a thorough study to optimize the reaction conditions, including measures to reduce the catalyst loading, lower the reaction temperature, and further generalize the substrate scope. We also performed mechanistic and computational investigations toward elucidating the catalytic cycle, active catalyst species, and the stereoelectronic effects on enantioselectivity of this reaction.

## Results

### 1. Effects of Water on Catalyst Turnover

In our initial report,<sup>13</sup> we were able to demonstrate that the addition of up to 10 equivalents of water had no deleterious effect. Despite this, water was not considered as an important additive in the initially reported conditions because the stoichiometric arylboronic acid was believed to be a sufficient proton source to turn over the catalyst. In considering the overall reaction scheme, a more precise analysis of the mass balance of the reaction led us to reconsider the importance of water as a participant in the overall transformation (Scheme 2a).

These considerations proved to be essential during the scale up of the reaction. Attempts to use the original conditions (with no water added) failed to convert enone **2** efficiently, generating the desired ketone (**3**) only in moderate yield (Scheme 2b). We reasoned that when the reaction is performed on a small scale under ambient atmosphere the moisture present in the air and on the glassware could be sufficient to drive the reaction to completion. On a larger scale, however, where a more significant quantity of water was necessary, this was no longer true. Gratifyingly, upon the addition of as little as 1.5 equivalents of water to the reaction mixture, both reactivity and the enantioselectivity were restored (Scheme 2c), affording ketone **3** in high yield and ee.

We next sought to measure deuterium incorporation at the carbonyl  $\alpha$ -position as a method to determine the source of the proton utilized in reaction turnover. Reactions were performed substituting deuterium oxide for water and observed by  $^1\text{H}$  and  $^2\text{H}$  NMR analysis (Figure 1). Using phenylboronic acid, the reaction afforded ketone **3** in similar yield and enantioselectivity (Figure 1a). Likewise, substitution of phenylboroxine ((PhBO) $_3$ ) for phenylboronic acid and deuterium oxide for water (Figure 1b) resulted in identical yield, albeit with slightly depressed ee observed in ketone **3**. Analysis of ketone **3** by  $^1\text{H}$  NMR (Figure 1c) showed significant deuterium incorporation at the  $\alpha$ -position of the carbonyl, even in the presence of phenylboronic acid.<sup>18</sup> As expected, a higher degree of deuterium incorporation was observed in the reaction where phenyl boroxine was substituted for the boronic acid, however, the similar level of incorporation in both experiments suggested that the deuterium oxide was the agent assisting reaction turnover regardless of the use of protic or aprotic boron reagent.

## 2. Effects of Salt Additives on Reaction Rate

Satisfied with our ability to perform the reaction on scale, we turned our attention toward improving the catalyst activity. We observed that nearly all previous literature reports regarding palladium-catalyzed conjugate addition utilized cationic precatalysts featuring weakly-coordinative anions (PF $_6^-$ , SbF $_6^-$ , BF $_4^-$  etc.). We reasoned that the substitution of the trifluoroacetate counterion with a less coordinative species could lead to an increase in reaction rate. With this goal in mind, we examined a series of salt additives containing weakly coordinative counterions. We viewed the strategy for the *in situ* generation of the catalyst as the more practical and operationally simple alternative to the design, synthesis, and isolation of a new dicationic palladium precatalyst.

We investigated a number of salt additives to test this mechanistic hypothesis (Table 1). Coordinating counterions like chloride (entry 1) shut down reactivity. Pleasingly, as per our hypothesis, weakly coordinating counterions with sodium cations (entries 2–4) facilitated swift reaction, albeit with depressed ee. Tetrabutylammonium salts (entries 5–6) encountered slow reaction times, but good enantioselectivity. Sodium tetraphenylborate (entry 7), however, failed to deliver appreciable quantities of the quaternary ketone **3**, as rapid formation of biphenyl was observed. Ammonium salts (entries 8–9) provided the desired blend of reaction rate and enantioselectivity. We concluded that the hexafluorophosphate anion (entry 9) gave the optimal combination of short reaction time with minimized loss of enantioselectivity.

Based on our previous observations regarding the beneficial nature of water as an additive, we next explored the combined effect of water and hexafluorophosphate counterions. We found addition of both water and ammonium hexafluorophosphate were the most successful for increasing reactivity (Table 2). Water alone is insufficient to alter reactivity (entry 1), though the use of water with 30 mol % ammonium hexafluorophosphate greatly reduced the reaction time (entry 2) to only 1.5 hours with minimal effect on yield or ee. Furthermore, this combination of additives allowed the reaction to proceed at temperatures as low as 25 °C with 5 mol % palladium and 6 mol % ligand, and lowering of catalyst loadings to only 2.5 mol % of palladium and 3 mol % ligand at 40 °C (entry 3). We determined that optimal conditions for the reaction with lower catalyst loading to be 5 equivalents of water, 30 mol % ammonium hexafluorophosphate at 40 °C (entry 4), conditions that reproduce the original result at milder temperature and lower catalyst loadings. The reaction was extraordinarily tolerant of the amount of water, with both 10 (entry 5) and 20 (entry 6) equivalents of water having minimal effect on the yield or ee. Loadings of ammonium hexafluorophosphate can be as low as 5 mol % (entry 7) or 10 mol % (entry 8) with reactions completed in 24 hours. Stoichiometric additive (entry 9) gave no additional benefit (entry 4). Thus, we optimized

the additive amounts to be 30 mol % ammonium hexafluorophosphate and 5 equivalents of water.

Though increased rates were observed at 60 °C, the newly-found ability to perform reactions at 40 °C promoted superior reactivity of many substrates (Table 3). In fact, many substrates that exhibited high enantioselectivities under the original 60 °C reaction conditions suffered from poor yields. Reacting these substrates at 40 °C with the addition of ammonium hexafluorophosphate and water promoted significantly higher isolated yields. Arylboronic acids containing halides, such as *m*-chloro- (**4a**) and *m*-bromophenylboronic acid (**4b**) reacted with good enantioselectivity, but each substrate was originally marred by low yield using our original conditions. However, when reacted under the newly optimized reaction conditions, the isolated yield for the addition of chlorophenylboronic acid increased from 55% to 96% and for bromophenylboronic acid from 44% to 86%. Even *m*-nitroboronic acid (**4c**) reacted with higher isolated yield. Notably, some *ortho*-substituted boronic acids, such as *o*-fluorophenylboronic acid (**4d**), reacted more successfully under the milder reaction conditions, leading to increased isolated yield of 70%.

### 3. Non-Linear Effect Correlation of Catalyst and Product Enantioenrichment

Despite optimization of catalytic conditions for this highly enantioselective process, we were unsure of the nature of the active catalyst. For example, some rhodium conjugate addition systems have been shown to involve trimeric ligand/metal complexes.<sup>19</sup> Furthermore, Lu and coworkers reported the use of the palladium dimer [(bpy)Pd(OH)]<sub>2</sub>•2BF<sub>4</sub> as a precatalyst for conjugate addition.<sup>12</sup> We aimed to rule out the *in situ* formation and kinetic relevance of such dimers in our system. In seeking to support our hypothesized monomeric ligand-metal complex, we performed a non-linear effect study to determine the relationship between the ee of the ligand and the ee of the generated product.<sup>20</sup> The endeavor was to exclude dimeric (ML)<sub>2</sub> complexes from kinetic relevance, clarifying the monomeric nature of the active catalyst.<sup>21</sup> Five reactions were performed using a catalyst with different level of enantiopurity (racemic, 20%, 40%, 60% and 80% ee), and the obtained enantioselectivities were plotted against ee of the catalyst mixture (Figure 2). The obtained data clearly demonstrates that a non-linear effect is not present, and this observation strongly supports the action of a single, monomeric (ML)-type Pd/PyOx catalyst as the kinetically relevant species.<sup>21</sup> While the precise nature of the active catalyst species is unknown, isolated (PyOx)Pd(OCOCF<sub>3</sub>)<sub>2</sub> serves as an identically useful precatalyst, delivering ketone **3** in 99% yield and 92% ee.<sup>22</sup>

### 4. Computational Investigations of the Reaction Mechanism

Despite the results of the non-linear effect study agreeing with the proposed monomeric Pd/PyOx catalyst, no formal exploration of the mechanism of this transformation has been reported. Our initial hypothesis concerning the mechanism of the Pd/PyOx-catalyzed asymmetric conjugate addition were well informed by the seminal work of Miyaura,<sup>23</sup> however, the heterogeneous nature of the reaction medium, undefined nature of the precise catalyst,<sup>24</sup> and complicating equilibrium of organoboron species make kinetic analysis and thorough mechanistic study extremely challenging.<sup>25</sup>

Previously, we performed density functional theory (DFT) calculations to investigate the mechanism of palladium-catalyzed conjugate addition of arylboronic acids to enones, explicitly studying a catalytic palladium(II)/bipyridine system in MeOH solvent similar to that developed by Lu.<sup>12,26,27</sup> Calculations indicated that the mechanism involves three steps: transmetalation, carbopalladation (i.e. alkene insertion), and protonation with MeOH. Monomeric cationic palladium complexes are the active species in the catalytic cycle. The carbopalladation is calculated to be the rate- and stereoselectivity-determining step (Scheme

3). Now, we have performed DFT investigations on the catalytic cycle of reactions with the Pd/PyOx manifold and the effects of substituents and ligand on reactivity and enantioselectivity. The calculations were performed at the theoretical level found satisfactory in our previous study of the Pd/bipyridine system. Geometries were optimized with BP86<sup>28</sup> and a standard 6–31G(d) basis set (SDD basis set for palladium). Solvent effects were calculated with single point calculations on the gas phase geometries with the CPCM solvation model in dichloroethane. All calculations were performed with Gaussian 03.<sup>29</sup>

The computed potential energy surface for the catalytic cycle is shown in Figure 3. To simplify the computations of the mechanisms, a model ligand, in which the *t*-Bu group on the *t*-BuPyOx ligand was replaced by H, was used in the calculations of the mechanisms and the full ligand was used in the calculations of enantioselectivities which will be discussed below. Calculations on the reaction mechanism with the full ligand scaffold, however, generated a similar reaction diagram, and the rate- and stereo-determining steps were unchanged (see Figure S4 in the Supporting Information). The first step involves transmetalation of cationic Pd(II)-phenylborate complex **6** to generate a phenyl palladium complex. Transmetalation requires a relatively low free energy barrier of 15.6 kcal/mol (**7-ts**) with respect to complex **6** and leads to a phenyl palladium complex (**8**). Complex **8** undergoes ligand exchange to form a more stable phenyl palladium-enone complex **12**, in which the palladium binds to the enone oxygen atom. Complex **12** isomerizes to a less stable  $\pi$  complex **13** and then undergoes carbopalladation of the enone (**14-ts**) to form the new carbon–carbon bond. The carbopalladation step requires an activation free energy of 21.3 kcal/mol (**12**  $\rightarrow$  **14-ts**), and is the stereoselectivity-determining step. The regioisomeric carbopalladation transition state **16-ts** requires 5.6 kcal/mol higher activation free energy than **14-ts**, indicating the formation of the  $\alpha$ -addition compound **17** is unlikely to occur. Coordination of one water molecule to **15** leads to a water-palladium enolate complex **18**, and finally facile hydrolysis of **18** via **19-ts** affords product complex **20**. Liberation of the product **3** from **20** and coordination with another molecule of phenyl boronic acid regenerates complex **6** to complete the catalytic cycle. The computed catalytic cycle demonstrates some similarities with the Pd/bipyridine system in our previous computational investigation, which also involves monomeric cationic palladium as the active species and a catalytic cycle of transmetalation, carbopalladation, and protonation (with MeOH instead of H<sub>2</sub>O).

We also considered an alternative pathway involving direct nucleophilic attack of the phenyl boronic acid at the enone while the Pd catalyst is acting as a Lewis acid to activate the enone and directs the attack of the nucleophile (**9-ts**, Figure 3). This alternative pathway requires an activation free energy of 58.9 kcal/mol, 43.3 kcal/mol higher than the transmetalation transition state **7-ts**. Thus, this alternative pathway was excluded by calculations.

## 5. Experimental and Computational Investigations of the Enantioselectivities

With the aforementioned optimized reaction conditions and computational elucidation of the mechanism and stereoselectivity-determining transition states, we explored the effects of ligand and substrate on enantioselectivities by both experiment and computations. The enantioselectivity-determining alkene insertion step involves a four-membered cyclic transition state, which adopts a square-planar geometry. When a chiral bidentate ligand, such as (*S*)-*t*-BuPyOx, is employed, there are four possible isomeric alkene insertion transition states. The 3D structures of the alkene insertion transition states in the reaction of 3-methyl-2-cyclohexenone with (*S*)-*t*-BuPyOx ligand are shown in Figure 4. In **1-TS-A** and **1-TS-B**, the phenyl group is *trans* to the chiral oxazoline on the ligand, and in **1-TS-C** and **1-TS-D**, the phenyl group is *cis* to the oxazoline. **1-TS-A**, which leads to the predominant

(*R*)-product, is the most stable as the *t*-Bu group is pointing away from other bulky groups. **1-TS-C** leads to the same enantiomer, but with an activation enthalpy 2.6 kcal/mol higher than **1-TS-A**. The difference is likely to result from steric effects between the *t*-Bu on the ligand and the phenyl group, as indicated by the C-H and C-C distances labeled in Figure 4. **1-TS-B** and **1-TS-D** lead to the minor (*S*)-product, which are ~ 3 kcal/mol less stable than **1-TS-A** as a result of the repulsions between the *t*-Bu on the ligand and the phenyl group. In **1-TS-B**, the cyclohexenone ring is *syn* to the *t*-Bu group on the ligand. The shortest H-H distance between the ligand and the enone is 2.30 Å, suggesting some steric repulsions. In contrast, no ligand-substrate steric repulsions are observed in **1-TS-A**, in which the cyclohexenone is *anti* to the *t*-Bu. **1-TS-A** is also stabilized by a weak hydrogen bond between the carbonyl oxygen and the hydrogen geminal to the *t*-Bu group on the oxazoline. The O-H distance is 2.16 Å. Therefore, the enthalpy of **1-TS-B** is 2.3 kcal/mol higher than that of **1-TS-A**. This corresponds to an ee of 94%, which is very similar to the experimental observation (93%). Enantioselectivities were computed from relative enthalpies of the transition states. The selectivities computed from Gibbs free energies are very similar and are given in the SI.

We then investigated the effects of substituents on the ligand, in particular, at the 4 position of the oxazoline. The activation enthalpies of four alkene insertion pathways and the computed and experimental ee for the reaction of 3-methyl-2-cyclohexenone and phenyl boronic acid are summarized in Table 4. The *t*-Bu substituted PyOx ligand is found to be the optimum ligand experimentally (Table 4, entry 1). Replacing *t*-Bu with smaller groups, such as *i*-Pr, *i*-Bu, or Ph, dramatically reduces the ee.

The bulky *t*-Bu substituent on the ligand is essential not only to discriminate the diastereomeric transition states **1-TS-A** and **1-TS-B**, but also fix the orientation of the ligand to point the chiral center *cis* to the cyclohexenone. The energy difference between **1-TS-C** and **1-TS-D**, in which the chiral center on the ligand is *trans* to the cyclohexenone, is diminished.

When the (*S*)-*i*-PrPyOx ligand is used, the alkene insertion transition states with phenyl *trans* to the oxazoline (**2-TS-A** and **2-TS-B**) are also preferred. Thus, the enantioselectivity is determined by the energy difference between **2-TS-A** and **2-TS-B**. The (*R*)-product (via **2-TS-A**) is favored with a computed ee of 67%, slightly higher than the experimental ee (40%). The optimized geometries of **2-TS-A** and **2-TS-B** are shown in Figure 5 and the activation energies of all four transition states are shown in Table 4, entry 2. The *i*-Pr substituted ligand manifests via similar steric effects to (*S*)-*t*-BuPyOx, with, as expected, slightly weaker steric control. The lower enantioselectivity is attributed to the weaker steric repulsions between the *i*-Pr and the cyclohexenone in **2-TS-B** than those with the *t*-Bu in **1-TS-B**. The shortest distance between the hydrogen atoms on the ligand and the cyclohexenone is 2.35 Å in **2-TS-B**, slightly longer than the H-H distance in **1-TS-B** (2.30 Å). Less steric repulsions with the (*S*)-*i*-PrPyOx lead to 2.8 kcal/mol lower activation barriers for **2-TS-B** compared to **1-TS-B**. The ligand steric effects on the activation energies of the major pathway **TS-A** are smaller; the *i*-Pr substituted **2-TS-A** is only 0.6 kcal/mol more stable than the *t*-Bu substituted **1-TS-A**.

Similarly, when the (*S*)-*i*-BuPyOx or (*S*)-PhPyOx ligands are used, the enantioselectivity is further decreased to 0.8 kcal/mol (52% ee) for (*S*)-*i*-BuPyOx and 1.0 kcal/mol (65% ee) for (*S*)-PhPyOx. (Table 4, entries 3 and 4). These results agree well with the experimental trend.

Electronically differentiated PyOx ligands were also studied, and the results are summarized in Table 5. Electron-withdrawing or donating groups at the 4-position of the PyOx ligand showed minimal effects on the activation barriers, and were calculated to have minimal

effect on product ee. With the electron-withdrawing CF<sub>3</sub> and the electron-donating OCH<sub>3</sub> on the 4-position of the ligand, the activation enthalpies of alkene insertion increase by only 0.3 kcal/mol and 0.1 kcal/mol, respectively. The calculated ee are essentially identical among these three ligands. Experimentally, depressed ee was observed with both the 4-CF<sub>3</sub> and the 4-OCH<sub>3</sub> substituted ligands (entries 5 and 6). This confirms that the enantioselectivity is mainly attributed to the ligand/substrate steric repulsions.

The transition state structures shown in Figure 5 indicate that the steric control mainly arises from the repulsion of the C<sub>α</sub>' hydrogens on the cyclohexenone with the ligand. We then investigated the effects of substitution at the α' position and replacement of the CH<sub>2</sub> group with O. The reactivity and enantioselectivity of the reactions of lactone (Table 6, entry 7) and α',α'-dimethylcyclohexenone (Table 6, entry 8) with the (*S*)-*t*-BuPyOx ligand were computed. The enantioselectivity of lactone is predicted to be lower than cyclohexenone. The enthalpy of **7-TS-B** is 1.8 kcal/mol higher than that of **7-TS-A**, corresponding to an ee of 88%. Experimentally, the ee of the lactone product is 59%, also significantly lower than that with cyclohexenone. The optimized geometries of **7-TS-A** and **7-TS-B** are shown in Figure 5b. Replacing the CH<sub>2</sub> group with O decreases the ligand–substrate steric repulsion in **7-TS-B** is smaller than that in **1-TS-B**. This results in decreased enantioselectivity.

Methyl substitution at the α' position of cyclohexenone increases the steric repulsion with the *t*-Bu group on the ligand. Computations predicted increased enantioselectivity with α',α'-dimethylcyclohexenone (99% ee, Table 6, entry 8).<sup>30</sup> However, experimentally, the ee is comparable with the reaction of 3-methylcyclohexenone.

We also considered the electronic effects of arylboronic acids on enantioselectivity (Table 7). Computations predicted that *para*-electron-withdrawing substituents lead to increases in the activation barrier in alkene insertion, probably due to the electrophilicity of the β-carbon of the enone, and thus are predicted to afford slightly decreased enantioselectivities. Both *para*-acetylphenylboronic acid (**9-TS-A**) and *para*-trifluoromethylphenylboronic acid (**10-TS-A**) are predicted to react with 92% ee. However, both excellent enantioselectivities (96% ee) and excellent yields (99% isolated yield) are observed experimentally. Thus, the electronic effects of phenyl substituents on enantioselectivities are minimal, though slightly increased enantioselectivities are observed experimentally with the use of electron-withdrawing substituents.

Permutations of the pyridinooxazoline ligand framework corroborate the calculated data and suggest that a number of factors affect enantioselectivity. First, the steric demand of the chiral group on the oxazoline greatly impacts the observed enantioselectivity in the reaction (Table 8). Only *t*-BuPyOx (**1**) yields synthetically tractable levels of enantioselectivity, while the less sterically demanding *i*-PrPyOx (**21**), PhPyOx (**22**), and *i*-BuPyOx (**23**) all exhibit greatly diminished selectivity. Oxazoline substitution patterns also affect enantioselectivity. Substitution at the 4-position appears to be required for high selectivity, as substitution at the 5-position yields practically no enantioselectivity (ligand **24**). Electronic variation in the PyOx framework was observed to have a large effect on the *rate* of the reaction but, disappointingly, led to depressed stereoselectivity. CF<sub>3</sub>-*t*-BuPyOx (**25**) afforded the conjugate addition product in 99% yield and 81% ee. Surprisingly, MeO-*t*-BuPyOx (**26**) afforded the product in similar yield and only 78% ee. Finally, substitution at the 6-position of the pyridine (ligands **27** and **28**) greatly diminished both reactivity and selectivity, perhaps due to hindered ligand chelation to palladium.

Thus, we have concluded that enantioselectivity is controlled by the steric repulsion between the substituent on the chiral pyridinooxazoline ligand and the cyclohexyl ring. The bulkier *t*-Bu substituent on the (*S*)-*t*-BuPyOx ligand leads to greater enantioselectivity than the



reactions with (*S*)-*i*-PrPyOx or (*S*)-PhPyOx. Similarly, substrates with less steric demand adjacent the carbonyl exhibit lower enantioselectivities; for example the reaction of a lactone substrate (Table 6, TS-7) yields lower enantioselectivity due to smaller repulsions between the lactone oxygen and the *t*-Bu group.

## 6. Experimental Investigation of Arylpalladium(II) Intermediates and Formation of the Key C–C Bond

Experiments aiming to corroborate the calculated mechanism have been performed. We sought to observe the formation of the key C–C bond between an arylpalladium(II) species and the enone substrate in the absence of exogenous phenylboronic acid. Complexes **29** were synthesized as an intractable mixture of isomers, and were treated with AgPF<sub>6</sub> *in situ* to generate the [(PyOx)Pd(Ph)]<sup>+</sup> cation. Gratifyingly, complexes **29** serve as a competent precatalyst at 5 mol % loading, and affords ketone **3** in 96% yield and 90% ee (Table 9, entry 1). Varying the amount of complex utilized in proportion with phenylboronic acid, however, leads to significant production of biphenyl above 5 mol % (Table 9, entries 2–5). Utilizing even 25 mol % (entry 2) resulted in significant increase in biphenyl production (16% yield), and reduction in yield of the desired ketone **3** to 79%. Increasing complex loadings to 45 and 65 mol % (entries 3 and 4) leads to negligible production of ketone **3**, and nearly quantitative formation of biphenyl relative to catalyst loading. Furthermore, attempts to use the complex as a stoichiometric reagent in the place of PhB(OH)<sub>2</sub> lead to no observed product (entry 5), and exclusive formation of biphenyl. We hypothesize that quantitative generation of the reactive arylpalladium cation intermediate in high relative concentration leads quickly to disproportionation and formation of biphenyl and palladium(0). Omission of the AgPF<sub>6</sub> in favor of 30 mol % NH<sub>4</sub>PF<sub>6</sub> leads to isolation of only 22% yield of the conjugate addition product (entry 6). Finally, a control experiment demonstrates that AgPF<sub>6</sub> is incapable of catalyzing the reaction itself (entry 7).<sup>31</sup> This control further supports the computational results, which indicate a transmetalation-based mechanism as opposed to a Lewis acid-catalyzed pathway.

Concerned by our inability to observe consistent product formation at 40 °C, we sought alternative experimental verification that a putative cationic arylpalladium(II) species is capable of reacting to form conjugate addition products. Thus, we performed the stoichiometric reaction of the isomeric phenyl palladium iodide complexes (**29**) with AgPF<sub>6</sub> and 3-methylcyclohexenone at cryogenic temperatures, allowing the mixture to warm slowly to room temperature before quenching with trifluoroethanol.<sup>32</sup> We observed both conjugate addition product and biphenyl, with the desired adduct (**3**) isolated in 30% yield (Scheme 4a). Curiously, the conjugate addition adduct was isolated in only 55% ee. We considered that the isomeric mixture of phenyl palladium iodide isomers formed configurationally stable cationic species at cryogenic temperature.<sup>33</sup> Repeating the experiment, we substituted triphenylphosphine for methylcyclohexenone and observed the reaction at low temperature utilizing <sup>1</sup>H and <sup>31</sup>P NMR (Scheme 4b). Indeed, two <sup>31</sup>P signals corresponding to phosphine-bound palladium(II) species (**30**) were observed at 28 and 34 ppm. No isomerization was observed upon warming the isomeric mixture to room temperature.<sup>34</sup> Indeed, we were able to isolate and characterize the mixture of arylpalladium-phosphine cations. With evidence for the configurationally stable arylpalladium cation, we rationalized the observed 55% ee for the direct reaction of mixture **29** with methylcyclohexenone corresponds directly to the isomeric ratio of the complex: a ratio of 1.3:1 represents a 56:44 ratio of isomers. Assuming that the major isomer reacts with 92% ee, and the minor isomer reacts with no stereoselectivity to give racemic products,<sup>35</sup> a net stereoselectivity of 53.7% ee would be predicted for the product. Presuming configurational stability of the arylpalladium(II) cation as suggested by the triphenylphosphine trapping experiment, the diminished enantioselectivity observed in this result is unsurprising. Thus, we have obtained

experimental verification of the key C–C bond forming event of the Pd/PyOx asymmetric conjugate addition occurring from a quantitative generated arylpalladium(II) cation in the presence of enone substrate and absence of an exogenous arylboronic acid.

## Summary and Discussion

Several experimental results have been described that support the DFT-calculated mechanism for the Pd/PyOx-catalyzed asymmetric conjugate addition of arylboronic acids to cyclic enone (Figure 4); specifically, the role of the palladium catalyst has been addressed. Calculations and previous experimental work by Miyaura on palladium-catalyzed conjugate addition suggest that a transmetallation event occurs to transfer the aryl moiety from the boronic acid species to the palladium catalyst.<sup>4</sup> Our calculations indicated that the Pd/PyOx system operates under a similar manifold, and demonstrated a significant energy difference (transmetallation is favored by over 40 kcal/mol, Figure 4) between the potential roles of the palladium catalyst, suggesting that the role of the palladium species is not simply that of a Lewis acid. Furthermore, it is difficult to rationalize the high degree of enantioselectivity imparted by the chiral palladium catalyst if it is assumed that the metal acts only as a Lewis acid and is not directly mediating the key C–C bond-forming step.<sup>36</sup> Finally, a number of Lewis- and  $\pi$ -acidic metal salts were substituted for palladium with no product observed, further indicating that palladium-catalyzed conjugate addition is likely not a Lewis acid-catalyzed process.<sup>37</sup>

While highly Lewis-acidic, the role of cationic palladium(II) is to provide a vacant coordination site for the enone substrate to approach the catalyst. The presence of a cationic intermediate is further supported by the observed rate acceleration of non-coordinating anionic additives such as  $\text{PF}_6^-$  and  $\text{BF}_4^-$  salts (Table 1). Conversely, the addition of coordinating anions, such as chloride, inhibited the reaction (Table 1, entry 1). This counterion effect was evident even from choice of palladium(II) precatalysts.<sup>13</sup> For instance,  $\text{Pd}(\text{MeCN})_2\text{Cl}_2$  was not a suitable precatalyst, nor were any palladium(II) halides. Additionally,  $\text{Pd}(\text{OAc})_2$  only afforded modest yield of conjugate adducts, whereas the less coordinating counterion present in  $\text{Pd}(\text{OCOCF}_3)_2$  afforded complete conversion.

Satisfied that the palladium catalyst was not acting as a Lewis acid, we next sought to demonstrate the viability of the hypothesized arylpalladium(II) species as a catalyst (Table 9, entries 1–5). While serving as a suitable precatalyst under reaction conditions, arylpalladium(II) mixture **29** failed to facilitate the conjugate addition reaction when used in stoichiometric quantities in the presence of  $\text{AgPF}_6$  (entry 5). We rationalize this outcome to be the result of the highly reactive nature of the quantitatively generated arylpalladium(II) cation. Significant biphenyl formation- occurring even under dilute conditions representative of the catalytic reaction itself-suggest that alternative reaction pathways, such as disproportionation, readily out compete the desired insertion reaction. This reactive nature of the arylpalladium(II) cation led us to propose performing the stoichiometric reactions at low temperatures (Scheme 4). Successfully demonstrating that the key C–C bond could be generated, albeit in modest yield, from  $(\text{PyOx})\text{Pd}(\text{Ph})(\text{I})$  (**29**) corroborates both the precise role of the arylpalladium(II) cation in the calculated mechanism as well as the transition state put forth in the calculations. However, the modest yield of this process and requisite cryogenic temperatures prompted, again, consideration of the role of the arylboronic acid.<sup>38</sup> Calculations suggest that the presence of boronic acids as Lewis basic entities may serve to stabilize these reactive intermediates under the reaction conditions (Figure 3, cationic arylpalladium **8**).<sup>39</sup> This suggestion is consistent with the successful use of arylpalladium(II) mixture **29** as a precatalyst in the presence of arylboronic acids (Table 9, entry 1).

Lastly, water (or another proton source) is required for efficient turnover of the reaction. Considerations of reaction scale (Scheme 2) and deuterium incorporation experiments (Figure 1) suggest that water is the likely protonation agent, despite numerous other protic sources in the heterogenous reaction mixture. Attempts to use other, miscible proton sources (MeOH, phenol, *t*-BuOH, etc.) typically resulted in 10–15% less enantioselectivity observed.<sup>40</sup> 2,2,2-Trifluoroethanol can be successfully substituted for water with minimal loss of enantioselectivity, however it affords no supplementary benefit and water is the preferred additive for all reactions.<sup>25</sup> Water in combination with NH<sub>4</sub>PF<sub>6</sub> serves to facilitate milder reaction conditions (Table 2), which in turn greatly increases the synthetic scope with respect to challenging arylboronic acid nucleophiles (Table 3). Synthetic yields were observed to double in many cases, greatly increasing the utility of these transformations. The functional group tolerance of the Pd/PyOx system is unprecedented for asymmetric conjugate addition; it encompasses a wide array of halides, carbonyl functional groups, protected phenols, acetamides, free hydroxyl groups, and even nitro groups. Many of these groups are incompatible with traditional rhodium- and copper-catalyzed conjugate additions due to the reactivity with the nucleophiles used or the strong coordination of the functional group to the metal catalyst.

The combined results described herein have allowed us to put forth the following catalytic cycle (Figure 6). The cationic catalyst, represented as (PyOx)Pd(X)(L) (**31**), undergoes transmetalation with an arylboronic acid to yield cationic (PyOx)Pd(Ar)(L) (**32**). Substrate coordination forms cationic arylpalladium(II) **33**, which undergoes rate and enantioselectivity-determining insertion of the aryl moiety into the enone  $\pi$ -system to afford C-bound palladium enolate **34**. Tautomerization to the O-bound palladium enolate (**35**), or direct protonolysis of the C-bound enolate (**34**), liberates the conjugate addition product (**3**) and regenerates a cationic palladium(II) species for reentry into the catalytic cycle.

## Conclusions

In conclusion, we have reported experimental and computational results that corroborate a single PyOx ligand/metal complex as the active catalytic species in the palladium-catalyzed asymmetric conjugate addition of arylboronic acids to enones for the construction of quaternary stereocenters. We have used computational models to rule out a suggested alternative mechanism in which the palladium catalyst is acting as a Lewis acid to activate the enone. The preferred mechanism involves formal transmetalation from boron to palladium, rate- and enantioselectivity-determining carbopalladation of the enone olefin by a cationic palladium species, and protonolysis of the resulting palladium-enolate. We have taken advantage of these mechanistic insights to develop a modified reaction system whereby the addition of water and ammonium hexafluorophosphate increase reaction rates, and can facilitate lower catalyst loadings. The modified conditions have opened the door to new substrate classes that were inaccessible by the initially published reaction conditions. Furthermore, we have demonstrated that this operationally simple reaction is tolerant of ambient atmosphere and capable of producing enantioenriched,  $\beta$ -quaternary ketones on multi-gram scale. The steric and electronic effects of the boronic acid and enone substrates and the ligand on enantioselectivities were elucidated by a combined experimental and computational investigation. The enantioselectivity is mainly controlled by the steric repulsion of the *t*-Bu substituent of the oxazoline on the ligand and the C $_{\alpha}$ ' position hydrogens of the cyclohexenone substrate in the alkene insertion transition state.

Further investigations of both the scope of this transformation and its application toward natural product synthesis are current underway in our laboratories.

## Supplementary Material

Refer to Web version on PubMed Central for supplementary material.

## Acknowledgments

The authors thank NIH-NIGMS (B.M.S., R01 GM080269–01, K.N.H. GM36700), NSF (K.N.H., CHE-0548209), Caltech, Amgen, the American Chemical Society Division of Organic Chemistry (predoctoral fellowship J.C.H.), the Swiss National Science Foundation (postdoctoral fellowship M.G.) and the Japan Society for the Promotion of Science (postdoctoral fellowship K.K.) for financial support. A.N.M is grateful for a research fellowship by the German National Academy of Sciences Leopoldina (LPDS 2011–12). Prof. Theodor Agapie (Caltech) is thanked for helpful discussions. Dr. David VanderVelde of the Caltech NMR facility is thanked for invaluable assistance with NMR experiments and helpful discussions. Lawrence Henling and Dr. Michael K. Takase (Caltech) are gratefully acknowledged for X-ray crystallographic structural determination. The Bruker KAPPA APEXII X-ray diffractometer was purchased via an NSF CRIF:MU award to the California Institute of Technology, CHE-0639094. The Varian 400 MHz NMR spectrometer at Caltech was purchased via an NIH grant (RR027690). Calculations were performed on the Hoffman2 cluster at UCLA and the Extreme Science and Engineering Discovery Environment (XSEDE), which is supported by the NSF.

## References

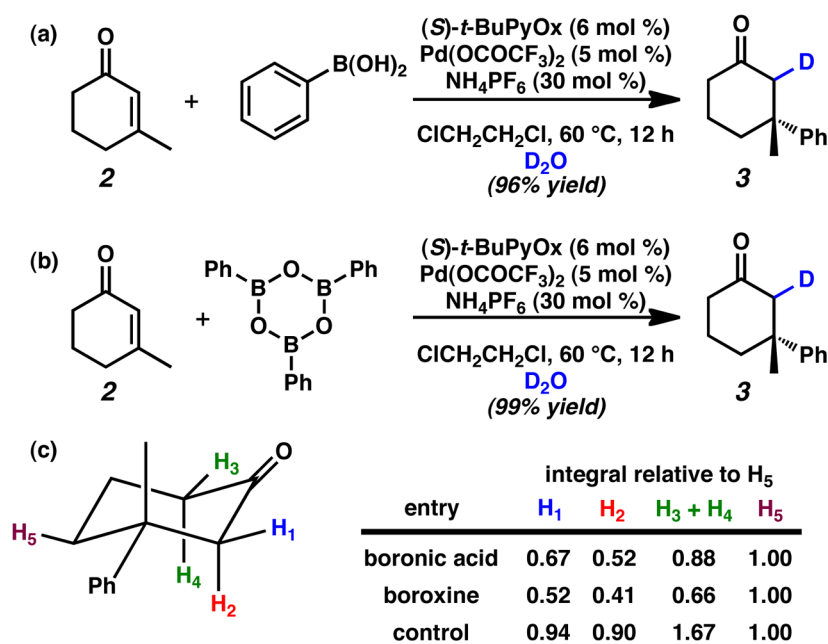
1. (a) Perlmutter, P. *Tetrahedron Organic Chemistry Series*. Vol. 9. Pergamon; Oxford: 1992. *Conjugate Addition Reactions in Organic Synthesis*. (b) Tomioka, K.; Nagaoka, Y. *Comprehensive Asymmetric Catalysis*. Jacobsen, EN.; Pfaltz, A.; Yamamoto, H., editors. Vol. 3. Springer-Verlag; New York: 1999. Chapter 31(c) Gini F, Hessen B, Feringa BL, Minnaard AJ. *Chem Commun*. 2007:710–712.
2. For reviews, see: Harutyunyan SR, den Hartog T, Geurts K, Minnaard AJ, Feringa BL. *Chem Rev*. 2008; 108:2824–2882. [PubMed: 18698733] Alexakis A, Backvall JE, Krause N, Pamies O, Dieguez M. *Chem Rev*. 2008; 108:2796–2893. [PubMed: 18671436] Lopez F, Minnaard AJ, Feringa BL. *Acc Chem Res*. 2007; 40:179–188. [PubMed: 17370989] Hayashi T, Yamasaki K. *Chem Rev*. 2003; 103:2829–2844. [PubMed: 12914482] Feringa BL. *Acc Chem Res*. 2000; 33:346–353. [PubMed: 10891052] Rossiter BE, Swingle NM. *Chem Rev*. 1992; 92:771–806.
3. (a) Shintani R, Duan WL, Hayashi T. *J Am Chem Soc*. 2006; 128:5628–5629. [PubMed: 16637617] (b) Hayashi T, Takahashi M, Takaya Y, Ogasawara M. *J Am Chem Soc*. 2002; 124:5052–5058. [PubMed: 11982369] (c) Takaya Y, Ogasawara M, Hayashi T. *J Am Chem Soc*. 1998; 120:5579–5580.
4. (a) Nishikata T, Yamamoto Y, Miyaura N. *Angew Chem, Int Ed*. 2003; 42:2768–2770. (b) Nishitaka T, Yamamoto Y, Miyaura N. *Chem Lett*. 2007; 36:1442–1443. (c) Nishitaka T, Kiyomura S, Yamamoto Y, Miyaura N. *Synlett*. 2008:2487–2490.
5. Gini F, Hessen B, Minnaard AJ. *Org Lett*. 2005; 7:5309–5312. [PubMed: 16268565]
6. For reviews on the synthesis of quaternary stereocenters, see: Denissova I, Barriault L. *Tetrahedron*. 2003; 59:10105–10146. Douglas CJ, Overman LE. *Proc Natl Acad Sci USA*. 2004; 101:5363–5267. [PubMed: 14724294] Christoffers J, Baro A. *Adv Synth Catal*. 2005; 347:1473–1482. Trost BM, Jiang C. *Synthesis*. 2006:369–396. Mohr JT, Stoltz BM. *Chem Asian J*. 2007; 21:1476–1491. [PubMed: 17935094] Cozzi PG, Hilgraf R, Zimmermann N. *Eur J Org Chem*. 2007:5969–5994.
6. For an excellent comprehensive review, see: Hawner C, Alexakis A. *Chem Commun*. 2010; 46:7295–7306.
7. (a) Wu J, Mampreian DM, Hoveyda AH. *J Am Chem Soc*. 2005; 127:4584–4585. [PubMed: 15796518] (b) Hird AW, Hoveyda AH. *J Am Chem Soc*. 2005; 127:14988–14989. [PubMed: 16248613] (c) Lee KS, Brown MK, Hird AW, Hoveyda AH. *J Am Chem Soc*. 2006; 128:7182–7184. [PubMed: 16734469] (d) Brown MK, May TL, Baxter CA, Hoveyda AH. *Angew Chem, Int Ed*. 2007; 46:1097–1100. (e) Fillion E, Wilsily A. *J Am Chem Soc*. 2006; 128:2774–2775. [PubMed: 16506736] (f) Wilsily A, Fillion E. *J Org Chem*. 2009; 74:8583–8594. [PubMed: 19824691] (g) Dumas AM, Fillion E. *Acc Chem Res*. 2010; 43:440–454. [PubMed: 20000793] (h) Wilsily A, Fillion E. *Org Lett*. 2008; 10:2801–2804. [PubMed: 18510334]
8. (a) d'Augustin M, Palais L, Alexakis A. *Angew Chem, Int Ed*. 2005; 44:1376–1378. (b) Vuagnoux-d'Augustin M, Alexakis A. *Chem–Eur J*. 2007; 13:9647–9662. [PubMed: 17849404] (c) Palais L,

- Alexakis A. *Chem–Eur J.* 2009; 15:10473–10485. [PubMed: 19718726] (d) Fuchs N, d’Augustin M, Humam M, Alexakis A, Taras R, Gladiali S. *Tetrahedron: Asymmetry.* 2005; 16:3143–3146. (e) Vuagnoux-d’Augustin M, Kehrli S, Alexakis A. *Synlett.* 2007:2057–2060. (f) May TL, Brown MK, Hoveyda AH. *Angew Chem, Int Ed.* 2008; 47:7358–7362. (g) Ladjel C, Fuchs N, Zhao J, Bernardinelli G, Alexakis A. *Eur J Org Chem.* 2009:4949–4955. (h) Palais L, Mikhel IS, Bournaud C, Micouin L, Falciola CA, Vuagnoux-d’Augustin M, Rosset S, Bernardinelli G, Alexakis A. *Angew Chem, Int Ed.* 2007; 46:7462–7465. (i) Hawner C, Li K, Cirriez V, Alexakis A. *Angew Chem, Int Ed.* 2008; 47:8211–8214. (j) Müller D, Hawner C, Tissot M, Palais L, Alexakis A. *Synlett.* 2010:1694–1698. (k) Hawner C, Müller D, Gremaud L, Felouat A, Woodward S, Alexakis A. *Angew Chem, Int Ed.* 2010; 49:7769–7772.
9. (a) Martin D, Kehrli S, d’Augustin M, Clavier H, Mauduit M, Alexakis A. *J Am Chem Soc.* 2006; 128:8416–8417. [PubMed: 16802804] (b) Kehrli S, Martin D, Rix D, Mauduit M, Alexakis A. *Chem–Eur J.* 2010; 16:9890–9904. [PubMed: 20540048] (c) Hénon H, Mauduit M, Alexakis A. *Angew Chem, Int Ed.* 2008; 47:9122–9124. (d) Matsumoto Y, Yamada KI, Tomioka K. *J Org Chem.* 2008; 73:4578–4581. [PubMed: 18489154]
10. (a) Shintani R, Tsutsumi Y, Nagaosa M, Nishimura T, Hayashi T. *J Am Chem Soc.* 2009; 131:13588–13589. [PubMed: 19728707] (b) Shintani R, Takeda M, Nishimura T, Hayashi T. *Angew Chem, Int Ed.* 2010; 49:3969–3971.
11. For excellent review articles, see: Gutnov A. *Eur J Org Chem.* 2008:4547–4554. Christoffers J, Koripelly G, Rosiak A, Rössle M. *Synthesis.* 2007:1279–1300.
12. Lin S, Lu X. *Org Lett.* 2010; 12:2536–2539. [PubMed: 20450192]
13. Kikushima K, Holder JC, Gatti M, Stoltz BM. *J Am Chem Soc.* 2011; 133:6902–6905. [PubMed: 21495647]
14. PyOx ligand scaffolds are increasingly common in asymmetric catalysis, see: Podhajsky SM, Iwai Y, Cook-Sneathen A, Sigman MS. *Tetrahedron.* 2011; 67:4435–4441. [PubMed: 21743752] Aranda C, Cornejo A, Fraile JM, García-Verdugo E, Gil MJ, Luis SV, Mayoral JA, Martínez-Merino V, Ochoa Z. *Green Chem.* 2011; 13:983–990. Pathak TP, Gligorich KM, Welm BE, Sigman MS. *J Am Chem Soc.* 2010; 132:7870–7871. [PubMed: 20486685] Jiang F, Wu Z, Zhang W. *Tetrahedron Lett.* 2010; 51:5124–5126. Jensen KH, Pathak TP, Zhang Y, Sigman MS. *J Am Chem Soc.* 2009; 131:17074–17075. [PubMed: 19902942] He W, Yip KT, Zhu NY, Yang D. *Org Lett.* 2009; 11:5626–5628. [PubMed: 19905004] Dai H, Lu X. *Tetrahedron Lett.* 2009; 50:3478–3481. Linder D, Buron F, Constant S, Lacour J. *Eur J Org Chem.* 2008:5778–5785. Schiffrer JA, Machotta AB, Oestreich M. *Synlett.* 2008:2271–2274. Koskinen AMP, Oila MJ, Tois JE. *Lett Org Chem.* 2008; 5:11–16. Zhang Y, Sigman MS. *J Am Chem Soc.* 2007; 129:3076–3077. [PubMed: 17298071] Yoo KS, Park CP, Yoon CH, Sakaguchi S, O’Neill J, Jung KW. *Org Lett.* 2007; 9:3933–3935. [PubMed: 17760452] Dhawan R, Dghaym RD, StCyr DJ, Arndtsen BA. *Org Lett.* 2006; 8:3927–3930. [PubMed: 16928040] Xu W, Kong A, Lu X. *J Org Chem.* 2006; 71:3854–3858. [PubMed: 16674059] Malkov AV, Stewart Liddon AJP, Ramírez-López P, Bendová L, Haigh D, Kocovsky P. *Angew Chem, Int Ed.* 2006; 45:1432–1435. Abrunhosa I, Delain-Bioton L, Gaumont AC, Gulea M, Masson S. *Tetrahedron.* 2004; 60:9263–9272. Brunner H, Kagan HB, Kreutzer G. *Tetrahedron: Asymmetry.* 2003; 14:2177–2187. Cornejo A, Fraile JM, García JI, Gil MJ, Herreras CI, Legarreta G, Martínez-Merino V, Mayoral JA. *J Mol Catal A: Chem.* 2003; 196:101–108. Zhang Q, Lu X, Han X. *J Org Chem.* 2001; 66:7676–7684. [PubMed: 11701020] Zhang Q, Lu X. *J Am Chem Soc.* 2000; 122:7604–7605. Perch NS, Pei T, Widenhofer RA. *J Org Chem.* 2000; 65:3836–3845. [PubMed: 10864772] Bremberg U, Rahm F, Moberg C. *Tetrahedron: Asymmetry.* 1998; 9:3437–3443. Brunner H, Obermann U, Wimmer P. *Organometallics.* 1989; 8:821–826.
15. The ligand was prepared as described in the literature, see: Brunner H, Obermann U. *Chem Ber.* 1989; 122:499–507. See Supporting Information for experimental details.
16. (a) Xu Q, Zhang R, Zhang T, Shi M. *J Org Chem.* 2010; 75:3935–3937. [PubMed: 20446712] (b) Zhang T, Shi M. *Chem–Eur J.* 2008; 14:3759–3764. [PubMed: 18307187] (c) Gottummukkala AL, Matcha K, Lutz M, de Vries JG, Minnaard AJ. *Chem–Eur J.* 2012; 18:6907–6914. [PubMed: 22532469]
17. Holder JC, Marziale AN, Gatti M, Mao B, Stoltz BM. *Chem–Eur J.* 2013; 19:74–77. [PubMed: 23208950]

18. We believe the small amount of deuterium incorporation at the methylene adjacent the enone occurs via substrate enolization during the extended reaction times under the mild reaction conditions.
19. Duan WL, Iwamura H, Shintani R, Hayashi T. *J Am Chem Soc.* 2007; 129:2130–2138. [PubMed: 17249670]
20. Guillaneux D, Zhao SH, Samuel O, Rainford D, Kagan HB. *J Am Chem Soc.* 1994; 116:9430–9439. Further evidence for the monomeric nature of the Pd/PyOx catalyst was provided by comparison of diffusion rates of various PyOx/Pd complexes by diffusion oriented spectroscopy (DOSY NMR). These studies suggest an upper bound for the molecular weight of the solution species of the catalyst, demonstrating that dimeric (ML)<sub>2</sub> complexes are not present. See Supporting Information.
21. (a) Inanaga J, Furuno H, Hayano T. *Chem Rev.* 2002; 102:2211–2226. [PubMed: 12059267] (b) Kagan HB. *Synlett.* 2001:888–899.(c) Girard C, Kagan HB. *Angew Chem, Int Ed.* 1998; 37:2922–2959.
22. For preparation and use of (PyOx)Pd(OCOCF<sub>3</sub>)<sub>2</sub> see Supporting Information.
23. Nishitaka T, Yamamoto Y, Miyaura N. *Organometallics.* 2004; 23:4317–4324.
24. The catalyst itself is known to be soluble and not zero valent palladium nanoparticles due to exclusion by a mercury drop test, see ref 17. For examples of the mercury drop test, see: Ines B, SanMartin R, Moure MJ, Dominguez E. *Adv Synth Catal.* 2009; 351:2124–2132. Ogo S, Takebe Y, Uehara K, Yamazaki T, Nakai H, Watanabe Y, Fukuzumi S. *Organometallics.* 2006; 25:331–338.
25. Attempts to study the reaction by NMR initially saw no reaction progress due to the inability to stir the immiscible reaction mixture in an NMR tube. Substitution of 2,2,2-trifluoroethanol for water as the super stoichiometric proton source facilitated the reaction to proceed in the absence of stirring with no detriment to the observed enantioselectivity, however the reaction was necessarily performed at sufficiently elevated temperature that observation of the initial rate was not tenable and, thus, kinetic study was abandoned.
26. Lan Y, Houk KN. *J Org Chem.* 2011; 76:4905–4909. [PubMed: 21539326]
27. For related computational studies on palladium-catalyzed conjugate additions of arylboronic acids to enones: Nishikata T, Yamamoto Y, Gridnev ID, Miyaura N. *Organometallics.* 2005; 24:5025–5032. Sieber JD, Liu S, Morken JP. *J Am Chem Soc.* 2007; 129:2214–2215. [PubMed: 17266312] Dang L, Lin Z, Marder TB. *Organometallics.* 2008; 27:4443–4454.
28. (a) Becke AD. *J Chem Phys.* 1993; 98:1372–1377.(b) Becke AD. *J Chem Phys.* 1993; 98:5648–5652.(c) Perdew JP, Chevary JA, Vosko SH, Jackson KA, Pederson MR, Singh DJ, Fiolhais C. *Phys Rev B.* 1992; 46:6671–6687.(d) Perdew JP. *Phys Rev B.* 1986; 33:8822–8824.
29. Frisch, MJ., et al. Gaussian 03, Revision C.02. Gaussian, Inc; Wallingford CT: 2004.
30. Here, it is assumed the isomeric *trans* and *cis* phenylpalladium complexes cannot undergo rapid isomerization before alkene insertion and thus the enantioselectivity is determined by the energy difference between **8-TS-A** and **8-TS-B**, since the transmetalation leading to the *trans* isomer is favored (see SI). If *trans/cis* isomerization is faster than alkene insertion, the enantioselectivity will be determined by the energy difference between **8-TS-A** and **8-TS-D** (98% *ee*).
31. Other Lewis acids also proved incapable of catalyzing the reaction, including AlCl<sub>3</sub> and Sn(OTf)<sub>2</sub>.
32. These experiments were followed by NMR (<sup>1</sup>H, <sup>13</sup>C), however no discrete intermediates were successfully characterized.
33. Attempts to separate the isomeric mixture of phenylpalladium iodide complexes failed by both conventional silica gel flash chromatography and preparatory HPLC.
34. Optimization of the *cis/trans* isomerization transition state of the cationic phenyl palladium(II) complex failed to locate a TS. Scan of the reaction coordinate indicates the barrier of isomerization is higher than 10 kcal/mol with respect to the cationic phenyl palladium complex **11**. This suggests the *cis/trans* isomerization via the dissociative mechanism via isomerization of the tri-coordinated complex **11** cannot occur. See Supporting Information for details.
35. Computations indicated that alkene insertion to the minor isomer of phenyl palladium complex, in which the Ph is *cis* to the oxazoline, yields very low enantioselectivity. The chiral oxazoline is

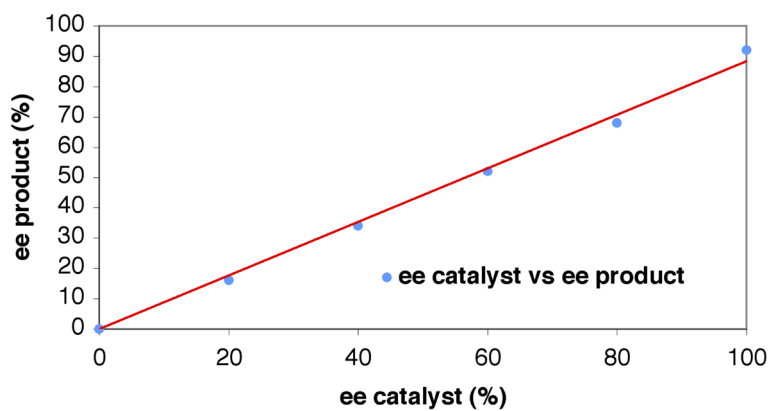
now *trans* to the enone, and thus the stereocontrol is diminished (see **1-TS-C** and **1-TS-D** in Figure 5).

36. A similar argument about imparted enantioselectivity can be made to rule out the catalytic activity of palladium(0) nanoparticles. Additionally, a mercury(0) poisoning test has ruled out the activity of palladium(0) nanoparticles in the Pd/PyOx manifold. See ref. 17.
37. Brønsted acid catalysis was also ruled out, as the substitution of trifluoroacetic acid for Pd(OCOCF<sub>3</sub>)<sub>2</sub> proved unable to catalyze the reaction. Protic acids are not tenable catalysts in the absence of palladium salts.
38. We have computed the effects of coordination with phenylboronic acid to activate the carbonyl on the enone in the alkene insertion step. No acceleration on alkene insertion was observed computationally with either Lewis acid or hydrogen bonding coordination. See Supporting Information.
39. The suggestion of boronic acid stabilization of arylpalladium cationic intermediates is consistent with the observation that boron species lacking hydroxyl groups serve as poor substrates for the reaction. For example, greatly diminished yields (and high degrees of biphenyl formation) are observed with the use of NaBPh<sub>4</sub> or KF<sub>3</sub>BPh as the phenyl donor species. See Supporting Information.
40. See Supporting Information of ref. 13 for details on the sensitivity of enantioselectivity of the Pd/PyOx system to polar, coordinating solvents. The addition of 5 equiv. of alcoholic co-solvent as a proton source is generally detrimental to the enantioselectivity and, occasionally, to the yield of the reaction.

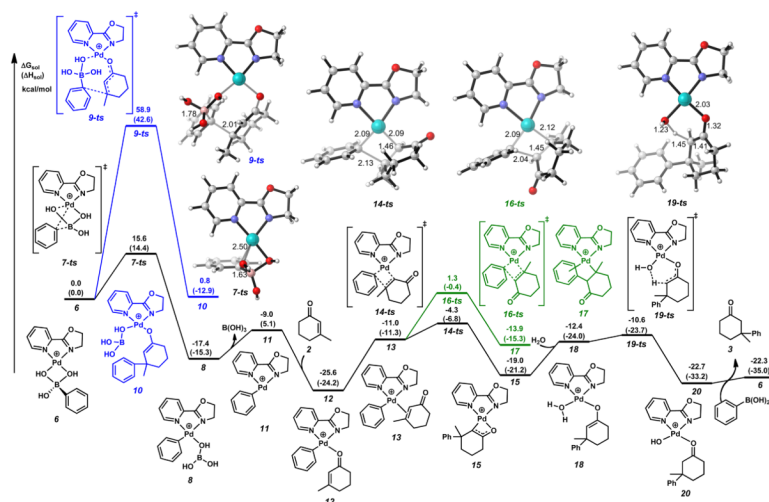


**Figure 1.** (a) deuterium incorporation using PhB(OH)<sub>2</sub>. (b) deuterium incorporation using (PhBO)<sub>3</sub>. (c) <sup>1</sup>H NMR data measuring deuterium incorporation by integral comparison of α-protons relative to H<sub>5</sub>, control: treatment of ketone **3** to deuterium incorporation conditions.

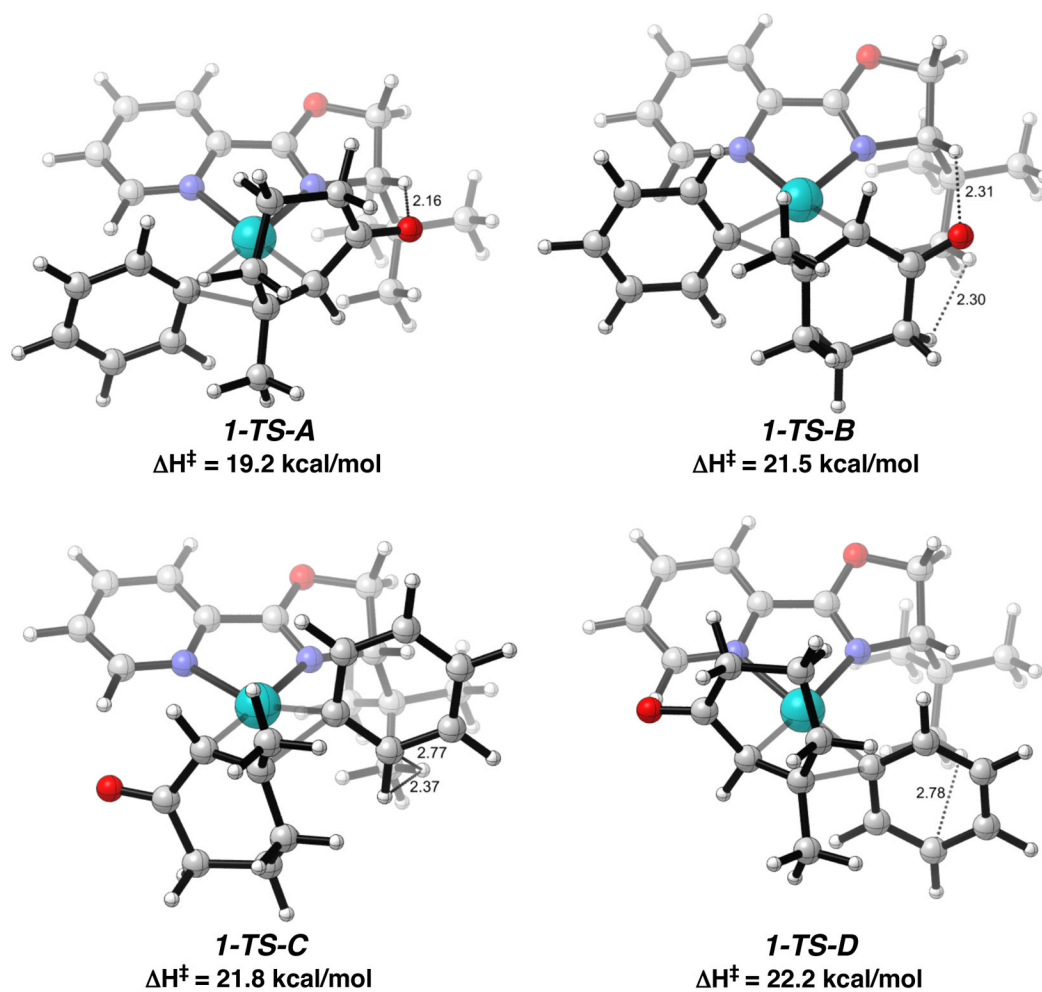




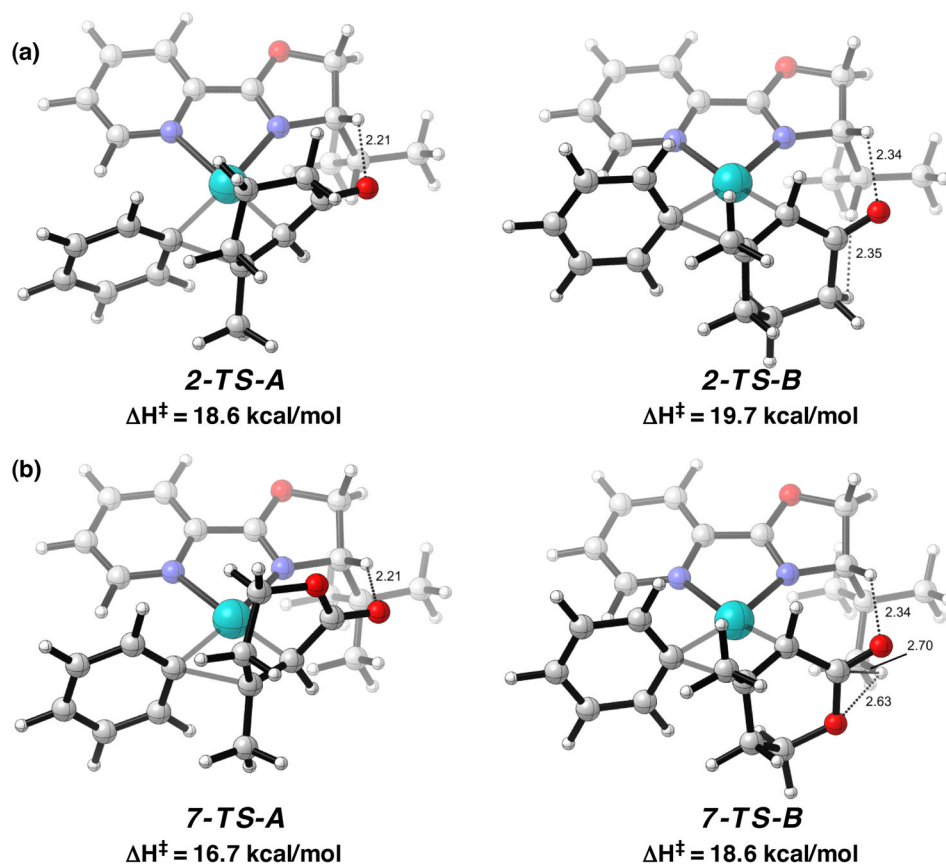
**Figure 2.**  
Determination of linearity between catalyst ee and product ee.



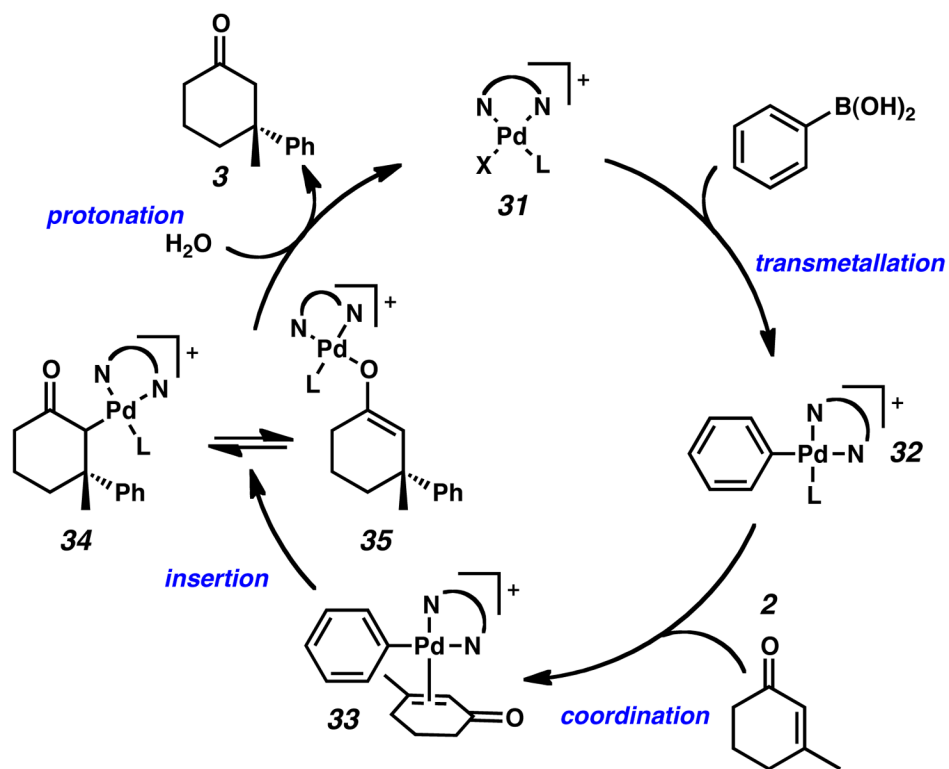
**Figure 3.** Computed potential energy surface of the catalytic cycle (shown in black), the alternative direct nucleophilic addition pathway (via **9-ts**, shown in blue), and the isomeric carbopalladation pathway (via **16-ts**, shown in green).



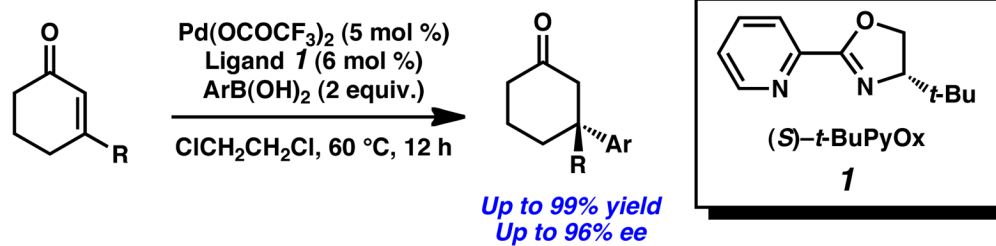
**Figure 4.** The optimized geometries of transition states in the enantioselectivity-determining alkene insertion step of the reaction of 3-methyl-2-cyclohexenone and phenyl boronic acid with (*S*)-*t*-BuPyOx ligand. Selected H–H, C–H, and O–H distances are labeled in Å.

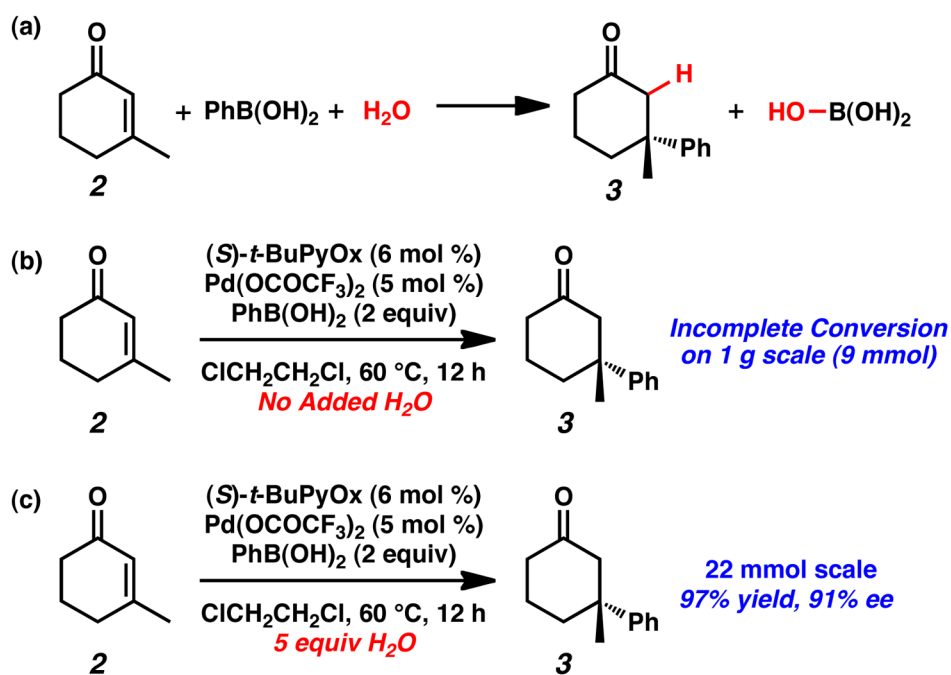


**Figure 5.** The optimized geometries of transition states in the enantioselectivity-determining alkene insertion step of the reaction of (a) 3-methyl-2-cyclohexenone and phenyl boronic acid with (*S*)-*i*-PrPyOx ligand; (b) 3-methyl- $\delta$ -2-pentenolide and phenyl boronic acid with (*S*)-*t*-BuPyOx ligand. Selected H–H, C–H, and O–H distances are labeled in Å.

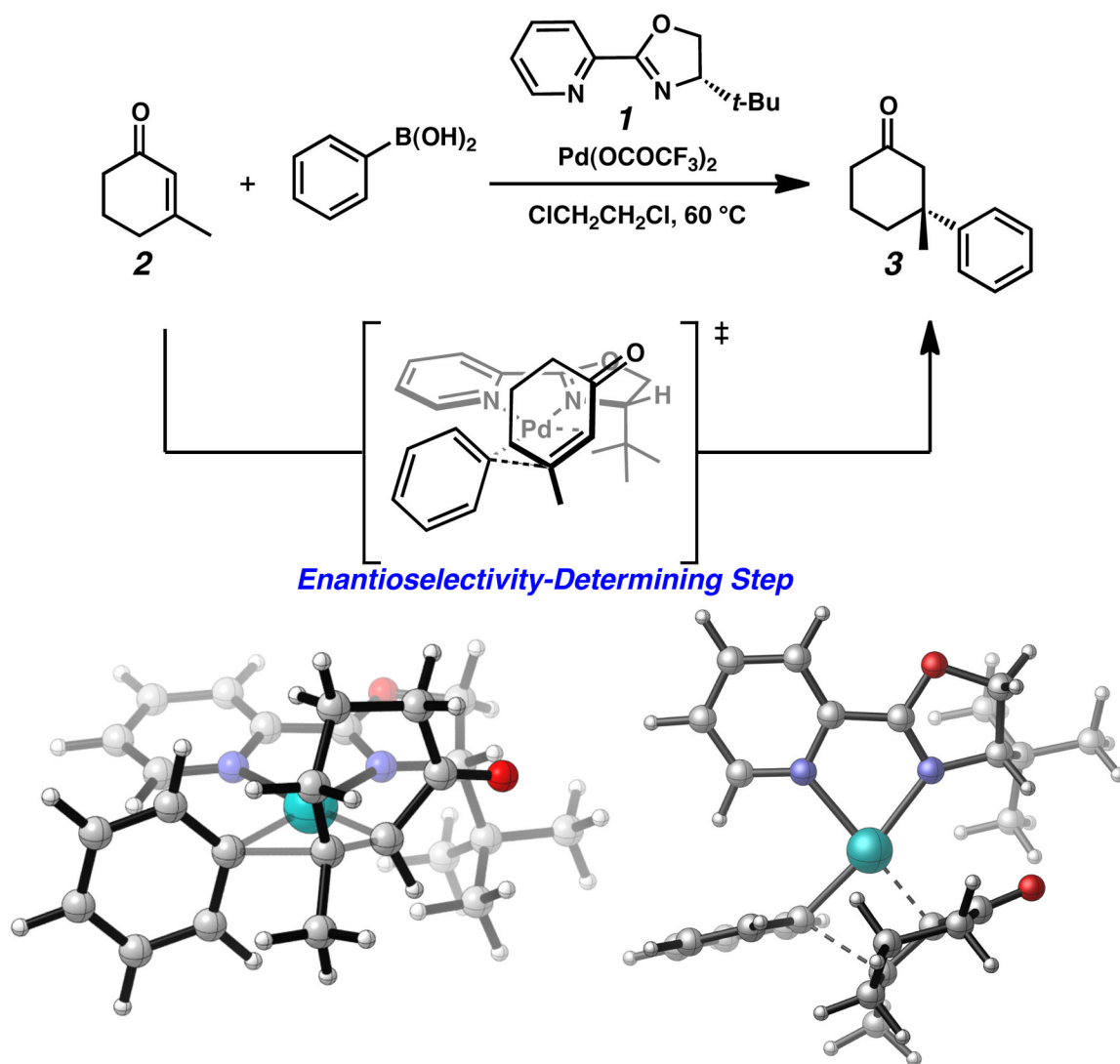


**Figure 6.** Proposed catalytic cycle for Pd/PyOx-catalyzed conjugate addition of arylboronic acids to cyclic enones.

**Scheme 1.**Asymmetric conjugate addition with (*S*)-*t*-BuPyOx ligand.

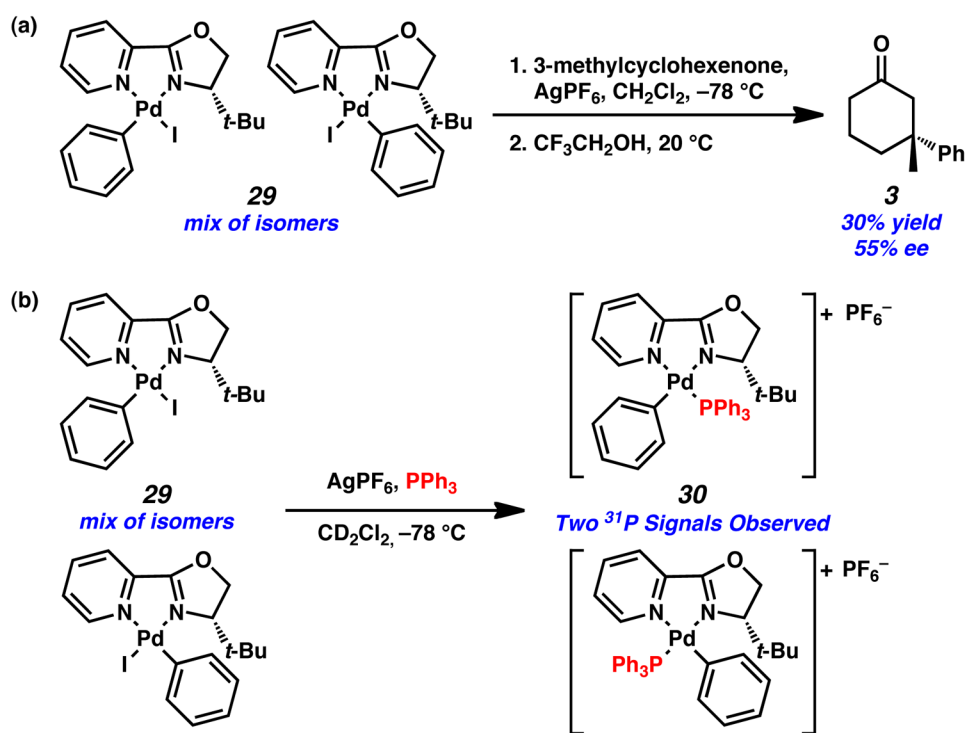
**Scheme 2.**

(a) Examination of reaction mass balance. (b) Absence of water prohibits scale-up. (c) Addition of water facilitates larger scale reactions.



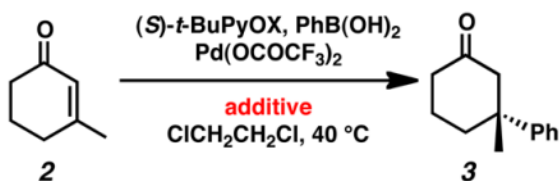
**Scheme 3.** Enantioselectivity-determining step in asymmetric conjugate addition of arylboronic acids to cyclic enones.



**Scheme 4.**

(a) Direct formation of C–C bond from arylpalladium(II) cation. (b) Triphenylphosphine trapping experiments demonstrates configurational stability of arylpalladium cation.

Table 1

Effect of salt additives on reaction rate.<sup>a</sup>

| entry <sup>a</sup> | additive                                    | time (h) | yield (%) <sup>b</sup> | ee (%) <sup>c</sup> |
|--------------------|---|----------|------------------------|---------------------|
| 1                  | NaCl  | 24       | trace                  | ---                 |
| 2                  | NaBF <sub>4</sub>                           | 8        | 81 <sup>d</sup>        | 88                  |
| 3                  | NaPF <sub>6</sub>                           | 6        | 97                     | 87                  |
| 4                  | NaSbF <sub>6</sub>                          | 5        | 99                     | 81                  |
| 5                  | <i>n</i> -(Bu) <sub>4</sub> PF <sub>6</sub> | 24       | 98                     | 90                  |
| 6                  | <i>n</i> -(Bu) <sub>4</sub> BF <sub>4</sub> | 24       | 95                     | 88                  |
| 7                  | NaBPh <sub>4</sub>                          | 24       | trace                  | ---                 |
| 8                  | NH <sub>4</sub> BF <sub>4</sub>             | 15       | 93                     | 89                  |
| 9                  | NH <sub>4</sub> PF <sub>6</sub>             | 12       | 96                     | 91                  |

<sup>a</sup> Conditions: phenylboronic acid (0.5 mmol), 3-methylcyclohexen-2-one (0.25 mmol), water (5 equiv), additive (30 mol %), Pd(OCOCF<sub>3</sub>)<sub>2</sub> (5 mol %) and (S)-*t*-BuPyOX (6 mol %) in ClCH<sub>2</sub>CH<sub>2</sub>Cl (1 mL) at 40 °C.

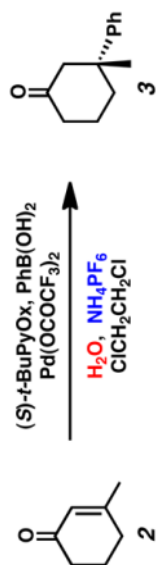
<sup>b</sup> GC yield utilizing tridecane standard.

<sup>c</sup> ee was determined by chiral HPLC.

<sup>d</sup> Reaction checked at 83% conversion as determined by GC analysis.

Table 2

Effect of water and  $\text{NH}_4\text{PF}_6$  on reaction rate.



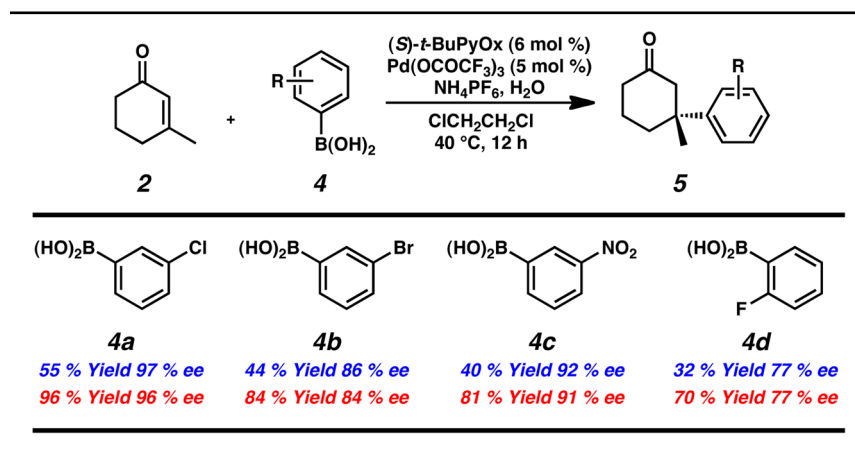
| entry <sup>a</sup> | $\text{H}_2\text{O}$ (equiv.) | $\text{NH}_4\text{PF}_6$ (mol %) | $\text{Pd}$ (mol %) | ligand (mol %) | temp ( $^\circ\text{C}$ ) <sup>b</sup> | time (h) | yield (%) <sup>b</sup> | ee (%) <sup>c</sup> |
|--------------------|-------------------------------|----------------------------------|---------------------|----------------|--|----------|------------------------|---------------------|
| 1                  | 10                            | ---                              | 5                   | 6              | 60                                     | 12       | 99                     | 91                  |
| 2                  | 5                             | 30                               | 5                   | 6              | 60                                     | 1.5      | 93                     | 88                  |
| 3                  | 5                             | 30                               | 5                   | 6              | 25                                     | 36       | 98                     | 91                  |
| 4                  | 5                             | 30                               | 2.5                 | 3              | 40                                     | 12       | 95                     | 91                  |
| 5                  | 10                            | 30                               | 2.5                 | 3              | 40                                     | 12       | 96                     | 89                  |
| 6                  | 20                            | 30                               | 2.5                 | 3              | 40                                     | 12       | 95                     | 90                  |
| 7                  | 5                             | 5                                | 2.5                 | 3              | 40                                     | 24       | 93                     | 90                  |
| 8                  | 5                             | 10                               | 2.5                 | 3              | 40                                     | 24       | 93                     | 92                  |
| 9                  | 5                             | 100                              | 2.5                 | 3              | 40                                     | 12       | 97                     | 88                  |

<sup>a</sup> Conditions: phenylboronic acid (1.0 mmol), 3-methylcyclohexen-2-one (0.5 mmol), water,  $\text{NH}_4\text{PF}_6$ ,  $\text{Pd(OCOCF}_3)_2$  and  $(S)$ -t-BuPyOx in  $\text{ClCH}_2\text{CH}_2\text{Cl}$  (2 mL).

<sup>b</sup> Isolated yield.

<sup>c</sup> ee was determined by chiral HPLC.

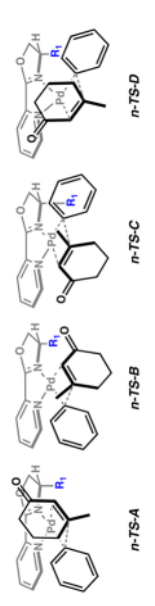
Table 3

Increased reaction yields with different arylboronic acid substrates under new reaction conditions.<sup>a</sup>

<sup>a</sup>Blue font: reported yield and ee of **5** in the absence of  $\text{NH}_4\text{PF}_6$  and water with reactions performed at 60 °C; red font: yield and ee of **5** with additives. Conditions: boronic acid (1.0 mmol), 3-methylcyclohexen-2-one (0.5 mmol),  $\text{NH}_4\text{PF}_6$  (30 mol %), water (5 equiv.),  $\text{Pd}(\text{OCOCF}_3)_2$  (5 mol %) and  $(S)$ -*t*-BuPyOx (6 mol %) in  $\text{ClCH}_2\text{CH}_2\text{Cl}$  (2 mL) at 40 °C. Isolated yield reported, ee was determined by chiral HPLC.

Table 4

Activation energies and enantioselectivities of alkene insertion with (S)-*t*-BuPyOX, (S)-*i*-PrPyOX, (S)-*i*-BuPyOX, (S)-PhPyOX, and (S)-PhPyOX ligands.



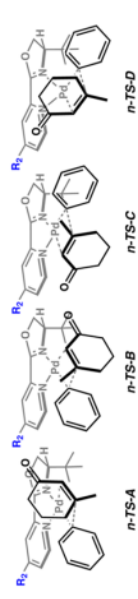
| TS | R <sup>1</sup> | ΔH <sup>‡</sup> <sup>a</sup> |      |      | ee <sup>b</sup> |           |
|----|----------------|------------------------------|------|------|-----------------|-----------|
|    |                | TS-A                         | TS-B | TS-C |                 |           |
| 1  | <i>t</i> -Bu   | 19.2                         | 21.5 | 21.8 | 22.2            | 94% [93%] |
| 2  | <i>i</i> -Pr   | 18.6                         | 19.7 | 20.1 | 20.0            | 67% [40%] |
| 3  | <i>i</i> -Bu   | 18.5                         | 19.3 | 20.4 | 20.4            | 52% [24%] |
| 4  | Ph             | 18.0                         | 19.0 | 19.6 | 20.2            | 65% [52%] |

<sup>a</sup>The values are activation enthalpies in kcal/mol calculated at the BP86/6-31G(d)-SDD level and the CPCM solvation model in dichloroethane.

<sup>b</sup>Experimental ee were obtained under standard conditions and are given in square brackets.

**Table 5**

Remote ligand substituent effects on activation energies and enantioselectivities of alkene insertion.



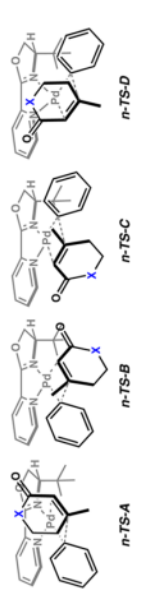
| TS       | R <sup>2</sup>   | ΔH <sup>‡</sup> <sup>a</sup> |             |      | ee <sup>b</sup> |           |
|----------|------------------|------------------------------|-------------|------|-----------------|-----------|
|          |                  | TS-A                         | TS-B        | TS-C |                 | TS-D      |
| <b>1</b> | H                | <b>19.2</b>                  | <b>21.5</b> | 21.8 | 22.2            | 94% [93%] |
| <b>5</b> | CF <sub>3</sub>  | <b>19.5</b>                  | <b>21.7</b> | 21.8 | 22.3            | 93% [81%] |
| <b>6</b> | OCH <sub>3</sub> | <b>19.3</b>                  | <b>21.5</b> | 21.5 | 22.2            | 93% [78%] |

<sup>a</sup>The values are activation enthalpies in kcal/mol calculated at the BP86/6-31G(d)-SDD level and the CPCM solvation model in dichloroethane.

<sup>b</sup>Experimental ee are given in square brackets.

Table 6

Activation energies and enantioselectivities of alkene insertion with substrates varying at the  $\alpha'$ -position.



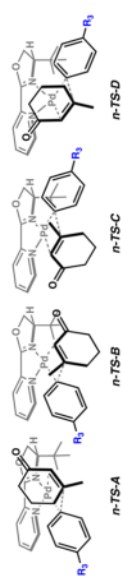
| TS | X                                | $\Delta H^\ddagger$ <sup>a</sup> |      |      | ee <sup>b</sup> |           |
|----|----------------------------------|----------------------------------|------|------|-----------------|-----------|
|    |                                  | TS-A                             | TS-B | TS-C |                 | TS-D      |
| 1  | CH <sub>2</sub>                  | 19.2                             | 21.5 | 21.8 | 22.2            | 94% [93%] |
| 7  | O                                | 16.7                             | 18.6 | 19.4 | 19.6            | 88% [57%] |
| 8  | C(CH <sub>3</sub> ) <sub>2</sub> | 17.9                             | 22.0 | 20.0 | 20.8            | 99% [90%] |

<sup>a</sup>The values are activation enthalpies in kcal/mol calculated at the BP86/6-31G(d)-SDD level and the CPCM solvation model in dichloroethane.

<sup>b</sup>Experimental ee are given in square brackets. Experimental isolated yields: TS-1: 99%, TS-7: 49%, TS-8: 9%.

Table 7

Activation energies and enantioselectivities of alkene insertion with various boronic acids.



| TS | R <sup>3</sup>     | $\Delta H^\ddagger$ <sup>a</sup> |      |      |      | ee <sup>b</sup> |
|----|--------------------|----------------------------------|------|------|------|-----------------|
|    |                    | TS-A                             | TS-B | TS-C | TS-D |                 |
| 1  | H                  | 19.2                             | 21.5 | 21.8 | 22.2 | 94% [93%]       |
| 9  | CH <sub>3</sub> CO | 21.6                             | 23.7 | 24.5 | 24.8 | 92% [96%]       |
| 10 | CF <sub>3</sub>    | 21.3                             | 23.4 | 23.6 | 24.2 | 92% [96%]       |

<sup>a</sup>The values are activation enthalpies in kcal/mol calculated at the BP86/6-31G(d)-SDD level and the CPCM solvation model in dichloroethane.

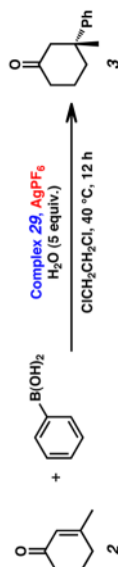
<sup>b</sup>Experimental ee are given in square brackets. Experimental isolated yields: TS-1: 99%, TS-9: 1%, TS-10: 99%, TS-11: 99%.





Table 9

Arylpalladium(II) catalyzed conjugate addition.<sup>a</sup>



| entry          | complex 29 (mol %) | AgPF <sub>6</sub> (mol %) | PhB(OH) <sub>2</sub> (mol %) | PhB(OH) <sub>2</sub> (mol %) | yield (%) |
|----------------|--------------------|---------------------------|------------------------------|------------------------------|-----------|
|                |                    |                           |                              |                              | 3         |
| 1              | 5                  | 10                        | 100                          | 100                          | 96        |
| 2              | 25                 | 50                        | 80                           | 80                           | 79        |
| 3              | 45                 | 90                        | 60                           | 60                           | 11        |
| 4              | 65                 | 130                       | 40                           | 40                           | 5         |
| 5              | 105                | 210                       | 0                            | 0                            | 0         |
| 6 <sup>b</sup> | 5                  | 0                         | 200                          | 200                          | 22        |
| 7              | 0                  | 20                        | 200                          | 200                          | 0         |

<sup>a</sup> Conditions: 3-methylcyclohexen-2-one (0.25 mmol), phenylboronic acid (equiv as stated), ClCH<sub>2</sub>CH<sub>2</sub>Cl (1 mL). Yields are isolated yields, ee determined by chiral HPLC.

<sup>b</sup> Reaction performed with 30 mol % NH<sub>4</sub>PF<sub>6</sub>